Nonlinear Dyn (2013) 73:1933–1943
DOI 10.1007/s11071-013-0914-8

ORIGINAL PAPER

Friction memory effect in complex dynamics of earthquake model

Srđan Kostić · Igor Franović · Kristina Todorović · Nebojša Vasović

Received: 20 December 2012 / Accepted: 15 April 2013 / Published online: 4 May 2013

Abstract In present paper, an effect of delayed frictional healing on complex dynamics of simple model of earthquake nucleation is analyzed, following the commonly accepted assumption that frictional healing represents the main mechanism for fault restrengthening. The studied model represents a generalization of Burridge–Knopoff single-block model with Dieterich–Ruina's rate and state dependent friction law. The time-dependent character of the frictional healing process is modeled by introducing time delay τ in the friction term. Standard local bifurcation analysis of the obtained delay-differential equations demonstrates that the observed model exhibits Ruelle–Takens–Newhouse route to chaos. Domain in parameters space where the solutions are stable for all values of time delay is determined by applying the Rouché theorem. The obtained results are corroborated by Fourier power spectra and largest Lyapunov exponents techniques. In contrast to previous research, the performed analysis reveals that even the small perturbations of the control parameters could lead to deterministic chaos, and, thus, to instabilities and earthquakes. The obtained results further imply the necessity of taking into account this delayed character of frictional healing, which renders complex behavior of the model, already captured in the case of more than one block.

Keywords Spring-block model · State variable · Time delay · Quasiperiodicity · Deterministic chaos

S. Kostić (✉) · N. Vasović
University of Belgrade Faculty of Mining and Geology, Đušina 7, 11000 Belgrade, Serbia
e-mail: srdjan.kostic@rgf.bg.ac.rs

I. Franović
University of Belgrade Faculty of Physics, Studentski trg 12, 11000 Belgrade, Serbia

K. Todorović
University of Belgrade Faculty of Pharmacy, Vojvode Stepe 450, 11000 Belgrade, Serbia

1 Introduction

There is a general consensus about the nucleation mechanism of tectonic earthquakes—these are produced when rock breaks suddenly in response to various geological forces [1]. The main role in this process is ascribed to rock strength and the size of accumulated strain energy. However, after a crack propagation, once a fault has been formed, its further motion is controlled by the friction between the interacting parts of Earth's crust [2]. It is this friction which determines whether the fault motion would be seismic or aseismic. In other words, depending on the frictional stability, the fault motion could eventually lead to earthquake.

The usual way of studying rock friction is by introducing friction constitutive laws, which emphasize the frictional instability as a possible mechanism for repetitive stick-slip failure and the seismic cycle [3].

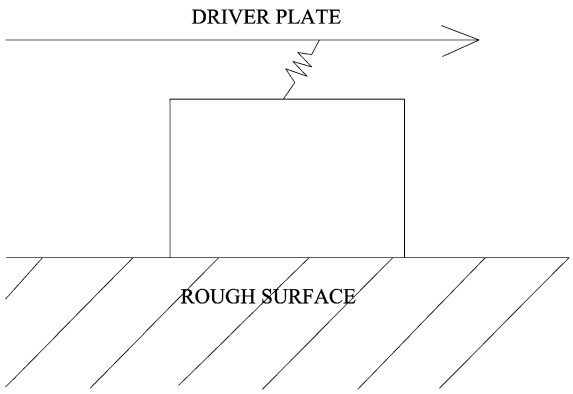

Fig. 1 The Burridge–Knopoff block and spring model, represented by a *slider* coupled through a *spring* to a *loader plate*

Since the Dieterich's original constitutive law [4], many laboratory-base friction laws were proposed, including Dieterich–Ruina or slowness law [4, 5]; Ruina's or slip law [5] and Perrin, Rice, and Zheng law [6]. The major problem of all these laws was the relation between static and dynamic friction. An elegant solution to this problem was introduced by Dieterich [4], who examined state variable as an average time of asperity contacts. Besides this interpretation, state variable was also considered as an average recent slip rate [7], surface separation rate [8] or surface temperature [5]. In our work, we simply analyze it as a function of the history of sliding, implying its time-dependent character, as already proposed in [9].

In present paper, Dieterich–Ruina law is used to model the frictional behavior of one-block Burridge–Knopoff model [10], which is today recognized as a common phenomenological model for earthquake nucleation mechanism. It consists of one block of a certain rock type, connected through harmonic spring to a moving plate and driven along the rough surface, which causes the whole system to move in a stick-slip fashion (Fig. 1). In the context of seismology, this physical system is analogous to a single fault patch of fixed dimensions that ruptures in an elastic medium [11, 12].

The inherent property of the Dieterich–Ruina rate- and state-dependent friction law is the logarithmic increase of frictional strength during the quasistationary contact between the block and the rough surface. This property corresponds well with seismic data, which also indicate that earthquake stress drop increases logarithmically with time [13, 14]. It is assumed that this fault strengthening between earthquakes is crucial for our understanding of the seismic cycle, and the physics of earthquake rupture [15].

This process of frictional restrengthening is mainly determined by the system's local memory of its effective contact time before slip arrest [16]. In other words, healing process during the quasistationary stage of the block motion primarily depends on the duration and, consequently, on the character of the contact between the moving block and the rough surface in the previous rapid stage of motion. In this paper, we introduce time delay τ, as an extension of the friction term, in order to describe this complex relation of two succeeding phases of the block motion, which are crucial for the stick-slip cycles and, hence, nucleation of frictional instabilities to occur. To our knowledge, the complex memory effect has not been considered so far by introducing the time delay in the equations governing the motion of spring-block model.

It is necessary to emphasize that this time delay effect is directly observed both in laboratory experiments and along the real fault. Laboratory experiments describing granite blocks sliding over a ground quartz (gouge) layer [15] were performed for the coseismic slip rates of 0.01^{-1} m/s and loading rates approximately equal to plate tectonic rates (30 mm/yr $\approx$ 3×10^{-9} m/s). According to the results of these laboratory tests, upon the cessation of motion, static friction shows an initial period of retarded healing for a few hundred days, after which an increase in healing is observed [15]. Moreover, it is determined that the length of this initial period of delayed healing varies with stiffness, which justifies our variation of the introduced time delay parameter τ. These laboratory results are further corroborated by seismic data, which indicate that there is a reduced healing rate during the period immediately following earthquakes of similar size ($<$10–100 days after the last earthquake), with small variations in stress drop.

We have to emphasize that this retarded initial period of fault healing irresistibly resembles the refractory stage of the relaxation oscillators. The usual way of modeling the behavior of such media is by using the delay differential equations, which is widely accepted method, particularly in the area of mathematical biology [17, 18].

Our goal is to determine the effect of the introduced time delay τ on the dynamical behavior of the spring-block model. Previously conducted research on the dynamics of spring-block model indicated the complex behavior of block motion. De Sousa Vieira [19]

showed that the two-block Burridge–Knopoff model in a symmetric configuration is chaotic. Erickson et al. [20] reported deterministic chaos in a one-block model, for rather large values of control parameters. Subsequently, the same authors [21] observed a transition from periodic behavior to chaos when the number of blocks is increased from 20 to 21. On the other hand, Pomeau and Le Berre [9] introduced additive noise to force chaos.

The scheme of this paper is as follows. In Sect. 2, we describe the system of equations in detail, including the original system. The main results are given in Sect. 3, where we introduce time delay in the system and analyze the extended model by applying the standard local bifurcation analysis. Here, we also apply Rouché theorem in order to determine the domain in the space of parameters where the stationary solutions are stable for any τ. The obtained complex dynamical behavior is confirmed through the calculation of the Fourier power spectra and the largest Lyapunov exponent. Concluding remarks are given in Sect. 5, together with the possible implications to earthquake phenomena and suggestions for further research.

2 Earthquake model

Our numerical simulations of a spring-block model are based on the system of equations proposed by Madariaga [20]. These equations of motion coupled with Dieterich–Ruina rate and state dependent friction law are originally given by:

$$\begin{aligned}\dot{\theta} &= -\left(\frac{v}{L}\right)\left(\theta + B\log\left(\frac{v}{v_0}\right)\right)\\ \dot{u} &= v - v_0\\ \dot{v} &= \left(-\frac{1}{M}\right)\left(ku + \theta + A\log\left(\frac{v}{v_0}\right)\right)\end{aligned} \tag{1}$$

where parameter M is the mass of the block and the spring stiffness k corresponds to the linear elastic properties of the rock mass surrounding the fault [2]. According to Dieterich and Kilgore [22], the parameter L corresponds to the critical sliding distance necessary to replace the population of asperity contacts. The parameters A and B are empirical constants, which depend on material properties. According to [23], parameter A measures the direct velocity dependence ("direct effect") while $(A - B)$ is a measure of the steady-state velocity dependence. For convenience, system (2) is nondimensionalized by defining the new variables θ', v', u', and t' in the following way: $\theta = A\theta'$, $v = v_0 v'$, $u = Lu'$, $t = (L/v_0)t'$, after which we return to the use of θ, v, u and t. This nondimensionalization puts the system into the following form:

$$\begin{aligned}\dot{\theta} &= -v\big(\theta + (1+\varepsilon)\log(v)\big)\\ \dot{u} &= v - 1\\ \dot{v} &= -\gamma^2\big[u + (1/\xi)\big(\theta + \log(v)\big)\big]\end{aligned} \tag{2}$$

where $\varepsilon = (B - A)/A$ measures the sensitivity of the velocity relaxation, $\xi = (kL)/A$ is the nondimensional spring constant, and $\gamma = (k/M)^{1/2}(L/v_0)$ is the nondimensional frequency [20].

3 Applied numerical methods

Owing to the apparent complexity of the considered systems of equations, the analytical solutions are not available even in the simplest case. Nonetheless, in terms of numerical treatment, one should note that the common logarithmic term renders the given systems extremely stiff in the plausible parameter domains, meaning that an exceedingly small iteration step is required to carry out the numerical integration. In particular, the step size is limited more severely by the stability than the accuracy requirement for the technique applied. This issue has earlier been resolved by introducing simplified versions of such systems, obtained by regularizing the nonlinear friction term for the near-zero velocities [24, 25]. However, it is quite likely that making these types of approximations may have been the determining factor for the scarce observations of chaos in the ensuing models if restricted to the realistic parameter values. For this reason, the objective has to be to select the numerical integration scheme allowing for the full nonlinear term to be retained. Therefore, instead of implementing some of the explicit methods that are bound to become unstable at some point, we adopt the backward differentiation formula (BDF) method, which belongs to the class of implicit integration schemes, already found useful in handling the stiff systems of differential equations [20]. In a nutshell, BDF is a linear multistep method that for the given function $y(t)$ and the moment τ_n approximates the function's derivative in terms of the $y(t)$ values at

τ_n and the earlier times, so to increase the accuracy of the approximation. Being implicit, BDF requires one to successively find solutions of nonlinear equations at each time step, this typically being accomplished by the modified Newton's method. For the considered system, we have implemented the second order algorithm, which links the function values at the given moment with the ones at two prior iteration steps.

As far as the analysis on local bifurcations is concerned, the considered ordinary-differentiation equation (ODE) and delay differentiation equation (DDE) systems are treated analytically, having the obtained results further corroborated by the appropriate numerical method. The latter involves the application of the software package DDE-BIFTOOL, which comprises a collection of adaptable Matlab routines suitable for the numerical bifurcation analysis of systems of delay differential equations [26, 27]. DDE-BIFTOOL has been successfully implemented in a number of different contexts, including biology, chemistry and physics [28, 29]. In order to determine the maximal Lyapunov exponent from the obtained time series, we have implemented the software for nonlinear time series analysis developed by Matjaž Perc. This piece of software relies on the well-known Wolf method for examining the given exponent's convergence in dependence on time. For further details and documentation one may refer to [30].

4 Extended model with time delay

The next step in the analysis of the frictional memory effect in generating the complex behavior of the spring-block model includes the introduction of time delay term τ in the nonlinear logarithmic friction term of the system (2), in which way we obtain the following system of delay differential equations:

$$\begin{aligned}\dot{\theta} &= -\nu\big[(\theta + (1+\varepsilon)\log\big(\nu(t-\tau)\big)\big]\\ \dot{u} &= \nu - 1\\ \dot{\nu} &= -\gamma^2\big[u + (1/\xi)\big(\theta + \log(\nu)\big)\big]\end{aligned} \tag{3}$$

The system (3) has only one stationary solution, namely $(\theta, u, v) = (0, 0, 1)$, which corresponds to steady sliding. We shall proceed in the standard way to determine and analyze the characteristic equation of (3) around a stationary solution $(0, 0, 1)$.

Linearization of the system (3) and substitution $\theta = Ae^{\lambda t}$, $u = Be^{\lambda t}$, $v = Ce^{\lambda t}$ and $v(t-\tau) = Ce^{\lambda(t-\tau)}$ results in a system of algebraic equations for the constants A, B, and C. This system has a nontrivial solution if the following is satisfied:

$$\begin{aligned}&-\lambda^3 - \lambda^2\left(\frac{\gamma^2}{\xi} + 1\right) - \lambda\gamma^2\left(\frac{1}{\xi} + 1\right) - \gamma^2\\ &\quad + \lambda(1+\varepsilon)\frac{\gamma^2}{\xi}e^{-\lambda\tau} = 0\end{aligned} \tag{4}$$

Equation (4) is the characteristic equation of the system (3). Infinite dimensionality of the system (3) is reflected in the transcendental character of (4). However, the spectrum of the linearization of Eqs. (3) is discrete and can be divided into infinite dimensional hyperbolic and finite dimensional non-hyperbolic parts [31, 32]. As in the finite dimensional case, the stability of the stationary solution is typically, i.e. in the hyperbolic case, determined by the signs of the real parts of the roots of (4). Exceptional roots, equal to zero or with zero real part, correspond to the finite dimensional center manifold where the qualitative features of the dynamics, such as local stability, depend on the nonlinear terms.

4.1 Stability for all values of time delay

Firstly, we outline answer to the question of stability of a stationary solution for all values of time delay τ and fixed values of the parameters. That is, we shall determine the domain in the space of parameters where the stationary solution is stable for any τ. To answer this question, one can invoke the theorem of Rouché [33], which states that: *If two functions*, $\psi(\lambda)$ *and* $\varphi(\lambda)$, *are analytic inside and on a closed contour* C, *and* $|\psi(\lambda)| < |\varphi(\lambda)|$ *on* C, *than* $\varphi(\lambda)$ *and* $\psi(\lambda) + \varphi(\lambda)$ *have the same number of zeros inside* C. In our case, the function $\varphi(\lambda)$ is related to the characteristic polynomial of the ODEs (3) and the function $\psi(\lambda) + \varphi(\lambda)$ is the characteristic function of the DDEs (5). The contour C consists of a part of the imaginary axes, containing the origin, and a stable contour C_R joining the end points of the part on the imaginary axes, and such that $R_z > 0$ for $z \in C_R$.

Thus, we have to estimate the parameters such that on the contour C,

$$\big|\varphi(\lambda)\big| > \big|\psi(\lambda)\big| \tag{5}$$

where

$$\phi(\lambda) = \lambda^3 + \lambda^2\left(\frac{\gamma^2}{\xi} + 1\right) + \lambda\gamma^2\left(\frac{1}{\xi} + 1\right) + \gamma^2$$
$$\psi(\lambda) = -\lambda(1+\varepsilon)\frac{\gamma^2}{\xi}e^{-\lambda\tau} \quad (6)$$

Nontrivial conditions on the parameters are obtained only on the pure imaginary part of the contour. The conditions of the Rouché theorem are fulfilled if

$$\xi > 2(1+\varepsilon) \quad (7)$$

Calculation in detail is given in the Appendix.

Thus, if (7) is satisfied than the stationary solution is stable for any value of the time delay. Outside the domain given by (7) stability of the stationary solution for nonzero time delay has to be investigated further. We shall seek for the relations $\tau = f(\gamma, \xi, \varepsilon)$ between the parameters and time delay such that some solutions of the characteristic equation (4) are pure imaginary $z = \pm i\omega$ with real and positive ω. Under some additional conditions [34], their relations may correspond to the Hopf bifurcation.

4.2 Local stability and bifurcations of the stationary solution

Equation (4) can be written in the following form:

$$\frac{-\lambda^3 - \lambda^2(\frac{\gamma^2}{\xi} + 1) - \lambda\gamma^2(\frac{1}{\xi} + 1) - \gamma^2}{\lambda(1+\varepsilon)\frac{\gamma^2}{\xi}} = -e^{-\lambda\tau} \quad (8)$$

in which we substitute $\lambda = i\omega$ to obtain:

$$\frac{i\omega^3 + \omega^2(\frac{\gamma^2}{\xi} + 1) - i\omega\gamma^2(\frac{1+\xi}{\xi}) - \gamma^2}{i\omega(1+\varepsilon)\frac{\gamma^2}{\xi}} = -(\cos\omega\tau - i\sin\omega\tau) \quad (9)$$

The resulting two equations for the real and imaginary part of (9) after squaring and adding give an equation for each of the parameters, ε and ξ in terms of the other parameters, ω and γ, and after division, an equation for τ in terms of the parameters ω, γ and ξ. In this way, one obtains parametric representations of the relations between τ and the parameters, which correspond to the bifurcation values $\lambda = i\omega$. The general form of such relations is illustrated by the following formula for ε as a function of ω:

$$\varepsilon = -1 + \sqrt{C} \quad (10)$$

where

$$C = \frac{[\omega^3 - \omega\gamma^2(\frac{1+\xi}{\xi})]^2 + [\omega^2(\frac{\gamma^2}{\xi} + 1) - \gamma^2]^2}{(\omega\frac{\gamma^2}{\xi})^2} \quad (11)$$

On the other hand, for ξ as a function of ω and τ:

$$\xi = \frac{[\omega\gamma^2\sin(\omega\tau) + \omega^2\gamma^2\cos(\omega\tau)]}{(\omega^3 - \omega\gamma^2)\sin(\omega\tau) + (\gamma^2 - \omega^2)\cos(\omega\tau)} \quad (12)$$

and for τ as a function of ω:

$$\tau = \tau_c = \frac{1}{\omega}\left[\text{arctg}\left(\frac{-\omega^2(\frac{\gamma^2}{\xi} + 1) + \gamma^2}{-\omega^3 + \omega\gamma^2(\frac{1+\xi}{\xi})}\right) + k\pi\right] \quad (13)$$

where k is any nonnegative integer such that $\tau_k \geq 0$.

Though the very form of the solution adopted for the characteristic equation is indicative of Hopf bifurcations, the rigorous proof of this claim is rather lengthy to convey [31, 35, 36]. Here, it suffices to say that the above parametric equations for ε, ξ, and τ coincide with the Hopf bifurcation curves illustrated in Figs. 2 and 3. In Fig. 2 are shown the bifurcation curves $\tau(\varepsilon)$ at the fixed parameter values $\xi = 0.5$ and $\gamma = 0.8$. The diagram displayed in Fig. 3 represents the bifurcation curves $\xi(\varepsilon)$, with the remaining parameters set to $\tau = 12$ and $\gamma = 0.8$. The system (4)

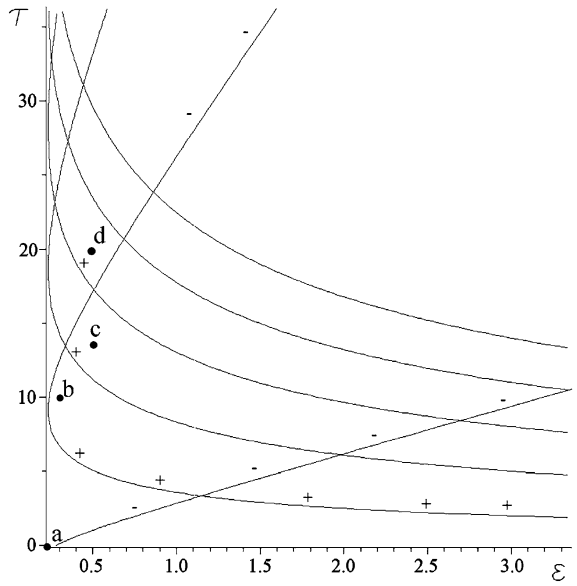

Fig. 2 Hopf bifurcation curves $\tau(\varepsilon)$, for the fixed values of parameters $\xi = 0.5$, and $\gamma = 0.8$. The *signs* $+/-$ denote the destabilizing (direct) or the stabilizing (inverse) Hopf bifurcations, respectively, as the delay is enhanced. The appropriate time series and the phase diagrams corresponding to points a, b, c, and d are shown in Fig. 4

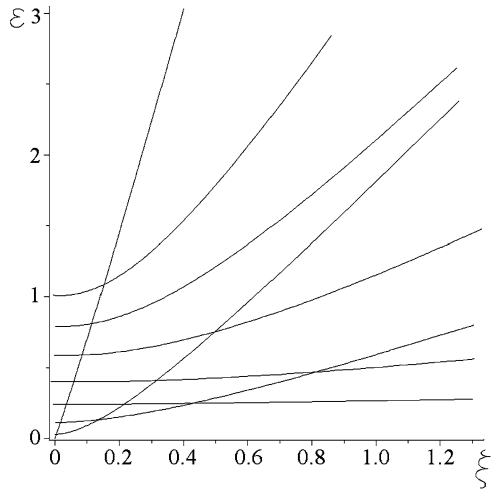

Fig. 3 Hopf bifurcation curves $\xi(\varepsilon)$ for the fixed values of parameters $\tau = 12$ and $\gamma = 0.8$

admits both the supercritical and the subcritical Hopf bifurcations, which is a matter less relevant for the present analysis. An issue of much greater importance is whether these bifurcations are of direct or the inverse type [37], the former (latter) resulting in creation (annihilation) of an unstable plane in the system's state space when the corresponding curve is crossed in the given direction. Put differently, the direct (inverse) bifurcations act in the destabilizing (stabilizing) fashion with respect to the underlying dynamics.

Since the main focus here lies with the effects of the time delay, we have examined more closely the sequence of bifurcations from Fig. 2, which the system undergoes in the direction of the increasing τ. To do so, one is required to determine the rate of change $\frac{d\,\mathrm{Re}(\lambda)}{d\tau}|_{\tau=\tau_c}$ of the real part of the root associated with the characteristic equation (4) as τ is changed through the critical values. In particular, if $d\,\mathrm{Re}(\lambda)/d\tau > 0$, the number of roots with the positive real part is increasing (destabilizing bifurcation), whereas the number decreases if the given derivative is negative (stabilizing bifurcation). The bifurcation curves in Fig. 2 are awarded the $+/-$ sign to reflect this point. Calculation of the above derivatives proceeds in the following way. Taking the derivative of the characteristic equation $\Delta(\lambda) = 0$, one first arrives at the relation $\frac{\partial \Delta}{\partial \lambda}\frac{d\lambda}{d\tau} + \frac{\partial \Delta}{\partial \tau} = 0$, which is for ease of calculation most conveniently applied in the form

$$\frac{d\tau}{d\lambda} = -\frac{\frac{\partial \Delta}{\partial \lambda}}{\frac{\partial \Delta}{\partial \tau}} \tag{14}$$

given that

$$\mathrm{sgn}\left(\frac{d\,\mathrm{Re}\,\lambda}{d\tau}\right)_{\tau=\tau_c} = \mathrm{sgn}\left(\mathrm{Re}\left(\frac{d\lambda}{d\tau}\right)^{-1}\right)_{\tau=\tau_c} \tag{15}$$

holds. Then, substituting for $\lambda = i\omega$ and extracting the real part, the final expression for the desired derivative reads

$$\mathrm{Re}\left(\frac{d\tau}{d\lambda}\right) = \frac{(-3\omega^2 + \gamma^2(\frac{1}{\xi}+1))(-\omega^3 + \omega\gamma^2(\frac{1}{\xi}+1)) - 2\omega(\frac{\gamma^2}{\xi}+1)(-\omega^2(\frac{\gamma^2}{\xi}+1)+\gamma^2)}{\omega^3(1+\varepsilon)^2(\frac{\gamma^2}{\xi})^2} - \frac{1}{\omega^2} \tag{16}$$

Beginning the analysis from the first curve encountered with the increasing delay, we report on an interesting finding that the associated derivatives are negative along the curve, meaning that the system undergoes an inverse bifurcation. In other words, the dynamic state of the system changes from oscillatory behavior to the stable stationary state. For comparison, see Fig. 4 where the temporal evolution and the phase portraits of the variable v are displayed for the fixed values of ε, ξ, γ and τ. The way in which the equilibrium regains stability with delay presents an instance of the time-delay induced amplitude death [38], the phenomenon which has been the subject of an intense research [39, 40]. This highlights the potentially intriguing role played by the small time delays, which may act to reduce the seismic activity, contributing to quenching of the possible major events. Nonetheless, reading from Fig. 2, one also learns that further increasing τ has a destabilizing effect on the fault dynamics. Not only can the delay cause the stationary state to become unstable triggering the periodic oscillations, but one may in fact find the bifurcation sequence that eventually leads to chaotic behavior. In particular, the system exhibits quasiperiodic (Ruelle–Takens–Newhouse) route to chaos [37, 41], such that after two supercritical Hopf bifurcations, the regular motion becomes highly unstable, eventually giving way to the dynamics, which falls onto the strange at-

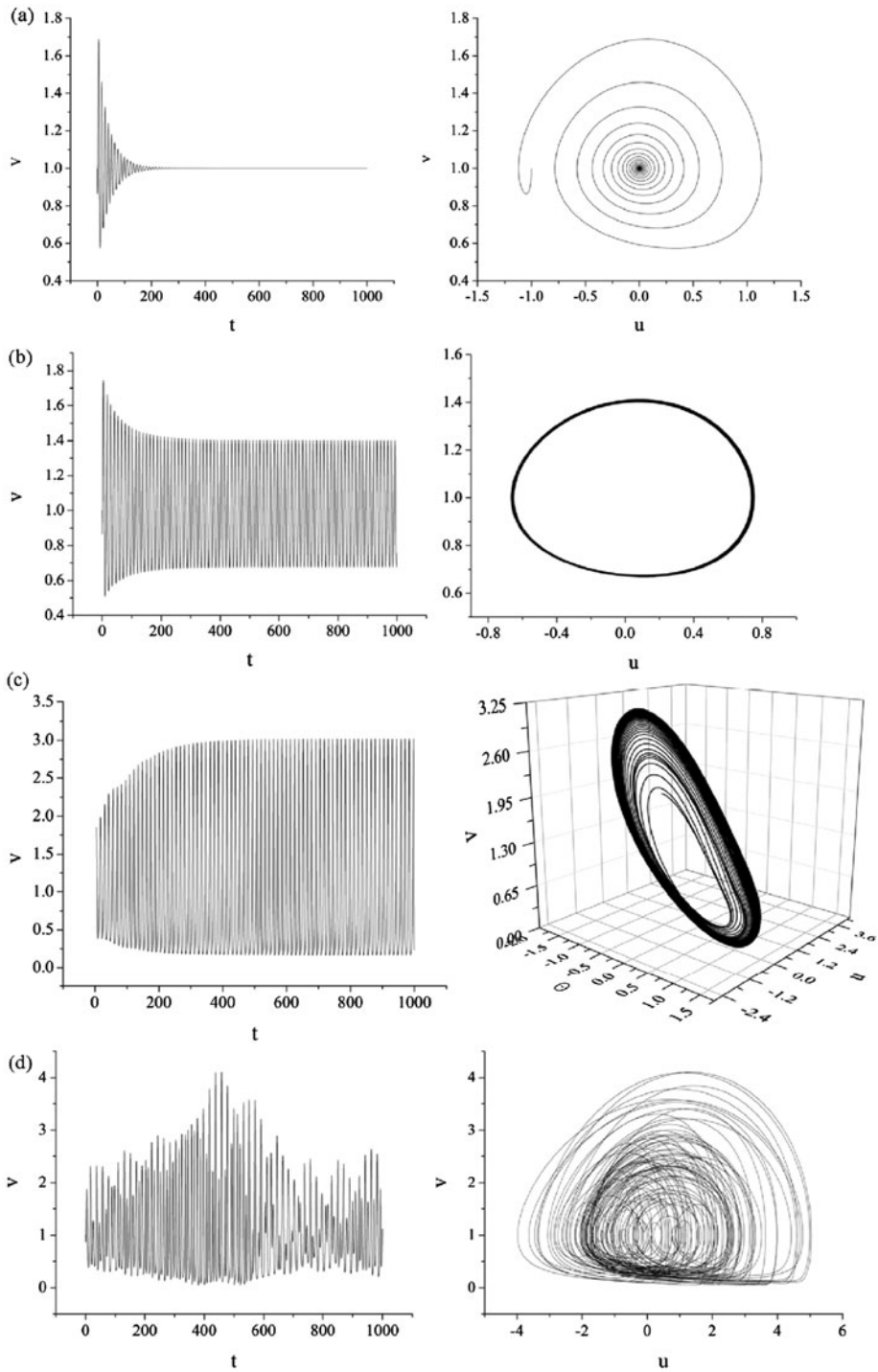

Fig. 4 Temporal evolution of variable v and the appropriate phase portraits for (**a**) $\tau = 0$, $\varepsilon = 0.2$, $\xi = 0.5$ and $\gamma = 0.8$ (fixed point); (**b**) $\tau = 10$, $\varepsilon = 0.3$, $\xi = 0.5$ and $\gamma = 0.8$ (oscillations); (**c**) $\tau = 13$, $\varepsilon = 0.5$, $\xi = 0.5$ and $\gamma = 0.8$ (torus); (**d**) $\tau = 20$, $\varepsilon = 0.5$, $\xi = 0.5$, and $\gamma = 0.8$ (chaos)

tractor. Apparently, only by increasing the time-lag τ, e.g., by setting $\tau = 0$, $\tau = 10$, $\tau = 13$ to $\tau = 20$, and by slightly changing the other parameter values, the block dynamics changes from the fixed point, over the limit cycle oscillation (first Hopf bifurcation) and torus (second Hopf bifurcation) to chaos.

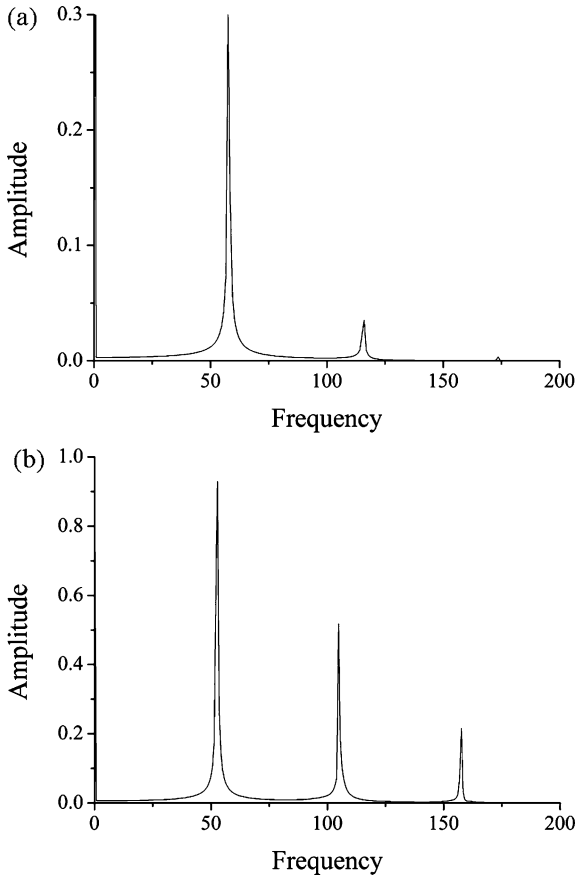

Fig. 5 (**a**) Single peak in power spectrum indicates the oscillatory behavior of the model. (**b**) Two peaks in power spectrum imply the appearance of torus (second Hopf bifurcation). The parameter values are the same as in Fig. 4(b) and 4(c), respectively

As apparent from previous analysis, in this case also, as in the case of periodically perturbed parameters, the onset of deterministic chaos is observed for significantly smaller values of ε (0.5) than those obtained in [20].

The scenario of deterministic chaos was further confirmed by calculation the Fourier power spectrum for oscillations, torus, and chaotic orbits, shown in Figs. 5 and 6, for the corresponding time series presented in Figs. 4(b), 4(c), and 4(d), respectively. The single peak in power spectrum in Fig. 5(a) indicates the oscillatory behavior of the system under study, while the second peak in Fig. 5(b) indicates a presence of torus. The broadband noise in Fig. 6 indicates that the attractor is strange.

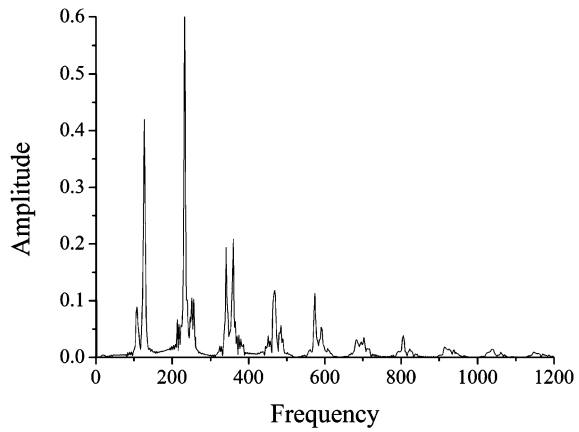

Fig. 6 The broadband noise in the Fourier power spectrum indicates the chaotic behavior of the system. The parameter values are identical to those in Fig. 4(d)

5 Concluding remarks

In this paper, we performed the analysis of variable delayed frictional healing on the dynamics of Burridge–Knopoff one-block model. The analysis was conducted by introducing time delay parameter τ in friction term. Standard bifurcation analysis of delayed differential equations is used to indicate the presence of the bifurcations from fixed point to periodic limit cycle and from periodic limit cycle into the quasi-periodic oscillations and, eventually, to deterministic chaos. These topological changes of dynamic states are obtained only by increasing the values of introduced time delay. However, the bifurcation analysis showed that for certain values of control parameters, the associated derivatives are negative along the curve, meaning that the system undergoes an inverse bifurcation, causing the dynamic state of the system to change from oscillatory behavior to the stable stationary state (time delay induced amplitude death). This feature is especially interesting, since it renders the possibility to suppress the occurrence of stick-slip frictional instability, and thus, the onset of seismic event. In the same time, we showed, by applying the Rouché theorem that for certain relations among the control parameters, the stationary solutions are stable for all values of time delay.

The main challenge in our analysis was the numerical stiffness of the examined system of differential equations, due to the nonlinear logarithmic term. This is why we used the software package DDE-BIFTOOL to corroborate our results obtained analytically.

We are aware of the fact that one-block model does not exactly describe all the main features of the earthquake nucleation mechanism, and, what is more, may exhibit some "exotic" dynamic features, which are not present along the real observed fault. However, the main outcomes of our analysis confirm the validity of the suggested modification of the existing models.

The primary outcome of this approach, in contrast to recent research, is that the onset of deterministic chaos is observed for much smaller values of the control parameter ε (0.5), which as it was already stated, models the ratio of long to short term stiffness in the model. This is in contrast to the research conducted by Erickson et al. [20], who observed the occurrence of deterministic chaos in Burridge–Knopoff model with one block for $\varepsilon = 11$. However, the results of our analysis correspond well with the subsequent research, also conducted by Erickson et al. [21], where the transition to chaos is observed as the number of block increases from 20 to 21, for the same value of parameter ε (0.5).

The second main outcome of our research is that the onset of chaos in the Burridge–Knopoff model with Dieterich–Ruina friction law is not size-dependent, which is in contrast to [21, 42]. Schmittbuhl et al. [42] also studied a spring-block model subject to a velocity weakening friction law and found that chaos was dependent on system size. Similarly, Erickson et al. [21] claimed that the critical value of the parameter ε necessary to induce chaos decreases as a function of the number of blocks. We believe that the neglecting of delayed nature of frictional healing and its role in dynamics of the spring-block model, in these previous research, prohibited the emergence of chaotic dynamics for smaller number of blocks, and, simultaneously, smaller values of parameter ε.

Concerning this, it could be said that we managed to fulfill the primary criterion of modeling—we reduced the complexity as much as possible, but still retained the main dynamical features of the model. Moreover, we showed that by introducing time delay in the friction term, complex dynamical behavior is achieved even in the case of one block Burridge–Knopoff model.

Following results of this research, it could be interesting to further examine the influence of delayed frictional healing in the model with two or three blocks. In this case, we could estimate the coupled effect of simultaneous perturbations of both parameter τ and spring stiffness k (connecting blocks), which would certainly generate more complex behavior.

Acknowledgements This research has been supported by the Ministry of Education, Science, and Technological development, Contracts Nos. 176016, 171015, and 171017.

Appendix

Starting from the system of equations:

$$\phi(\lambda) = \lambda^3 + \lambda^2\left(\frac{\gamma^2}{\xi} + 1\right) + \lambda\gamma^2\left(\frac{1}{\xi} + 1\right) + \gamma^2$$

$$\psi(\lambda) = -\lambda(1+\varepsilon)\frac{\gamma^2}{\xi}e^{-\lambda\tau}$$

one could obtain:

$$\begin{aligned}
\phi(\lambda) &= (\lambda+1)\left(\lambda^2 + \lambda\left(\frac{\gamma^2}{\xi}+1\right)\right) - \lambda^2 \\
&\quad - \lambda\left(\frac{\gamma^2}{\xi}+1\right) + \lambda\gamma^2\left(\frac{1}{\xi}+1\right) + \gamma^2 \\
&= (\lambda+1)\left(\lambda^2 + \lambda\left(\frac{\gamma^2}{\xi}+1\right)\right) \\
&\quad - (\lambda+1)\left(\lambda + \left(\frac{\gamma^2}{\xi}+1\right)\right) + \lambda \\
&\quad + \left(\frac{\gamma^2}{\xi}+1\right) + (\lambda+1)\left(\gamma^2\left(\frac{1}{\xi}+1\right)\right) \\
&\quad - \gamma^2\left(\frac{1}{\xi}+1\right) + \gamma^2 \\
&= (\lambda+1)\left(\lambda^2 + \lambda\left(\frac{\gamma^2}{\xi}+1\right) - \lambda - \left(\frac{\gamma^2}{\xi}+1\right)\right. \\
&\quad \left. + 1 + \gamma^2\left(\frac{1}{\xi}+1\right)\right) + \frac{\gamma^2}{\xi} - \frac{\gamma^2}{\xi} - \gamma^2 + \gamma^2 \\
&= (\lambda+1)\left(\lambda^2 + \lambda\left(\frac{\gamma^2}{\xi}+1\right) - \lambda\right) \\
&\quad - \left(\frac{\gamma^2}{\xi} + 1 - 1 - \frac{\gamma^2}{\xi} - \gamma^2\right) \\
&= (\lambda+1)\left(\lambda^2 + \lambda\left(\frac{\gamma^2}{\xi}+1\right) - \lambda + \gamma^2\right) \\
&= (\lambda+1)\left(\lambda^2 + \lambda\frac{\gamma^2}{\xi} + \gamma^2\right) \\
&= (\lambda+1)\left(\lambda - \frac{-\gamma^2 + \gamma\sqrt{(\gamma-2\xi)(\gamma+2\xi)}}{2\xi}\right) \\
&\quad \times \left(\lambda - \frac{-\gamma^2 - \gamma\sqrt{(\gamma-2\xi)(\gamma+2\xi)}}{2\xi}\right)
\end{aligned}$$

$$\geq |\lambda+1|\left|\frac{-\gamma^2-\gamma\sqrt{(\gamma-2\xi)(\gamma+2\xi)}}{2\xi}\right| \times \left|\frac{-\gamma^2+\gamma\sqrt{(\gamma-2\xi)(\gamma+2\xi)}}{2\xi}\right| = |\lambda+1|\gamma^2$$

Thus, we have:

$$\left|\phi(\lambda)\right| \geq |\lambda+1|\gamma^2$$

While for the $\psi(\lambda)$, we obtain:

$$\begin{aligned}\left|\psi(\lambda)\right| &= \left|-(\lambda+1)(1+\varepsilon)\frac{\gamma^2}{\xi}e - \lambda\tau + (1+\varepsilon)\frac{\gamma^2}{\xi}e^{-\lambda\tau}\right| \\ &\leq \left|(\lambda+1)(1+\varepsilon)\frac{\gamma^2}{\xi}e^{-\lambda\tau}\right| + \left|(1+\varepsilon)\frac{\gamma^2}{\xi}e^{-\lambda\tau}\right| \\ &= (\lambda+1)(1+\varepsilon)\frac{\gamma^2}{\xi} + (1+\varepsilon)\frac{\gamma^2}{\xi}\end{aligned}$$

i.e. $$\left|\phi(\lambda)\right| \geq |\lambda+1|\gamma^2 > |\lambda+1|(1+\varepsilon)\frac{\gamma^2}{\xi} + (1+\varepsilon)\frac{\gamma^2}{\xi}$$

assuming that $|\varphi(\lambda)| > |\psi(\lambda)|$ on the contour C.

Thus, according to the previous:

$$\begin{aligned}&\left|\phi(\lambda)\right| \\ &\geq |\lambda+1|\gamma^2 > |\lambda+1|(1+\varepsilon)\frac{\gamma^2}{\xi} + (1+\varepsilon)\frac{\gamma^2}{\xi} \\ &\geq \left|\psi(\lambda)\right| \quad\Rightarrow\quad |\lambda+1|\left(\gamma^2 - (1+\varepsilon)\frac{\gamma^2}{\xi}\right) \\ &> (1+\varepsilon)\frac{\gamma^2}{\xi} \quad\Rightarrow\quad |\lambda+1|\left(\gamma^2 - (1+\varepsilon)\frac{\gamma^2}{\xi}\right) \\ &\geq 1\left(\gamma^2 - (1+\varepsilon)\frac{\gamma^2}{\xi}\right) > (1+\varepsilon)\frac{\gamma^2}{\xi} \\ &\Rightarrow\quad \gamma^2 > 2(1+\varepsilon)\frac{\gamma^2}{\xi} \quad\Rightarrow\quad \xi > 2(1+\varepsilon)\end{aligned}$$

References

1. Bolt, A.B.: Earthquakes. Freeman, New York (2003)
2. Scholz, C.H.: The Mechanics of Earthquakes and Faulting. Cambridge University Press, Cambridge (2002)
3. Marone, C.: Laboratory derived friction laws and their application to seismic faulting. Annu. Rev. Earth Planet. Sci. **26**, 643–696 (1998)
4. Dieterich, J.H.: Modeling of rock friction: 1; experimental results and constitutive equations. J. Geophys. Res. **84**, 2161–2168 (1979)
5. Ruina, A.L.: Slip instability and state variable friction laws. J. Geophys. Res. **88**, 10359–10370 (1983)
6. Perrin, G., Rice, J.R., Zheng, G.: Self-healing slip pulse on a frictional surface. J. Mech. Phys. Solids **43**, 1461–1495 (1995)
7. Rabinowicz, E.: The intrinsic variables affecting the stick-slip process. Proc. Phys. Soc. Lond. **71**, 668–675 (1958)
8. Tolstoi, D.M.: Significance of the normal degree of freedom and natural normal vibrations in contact friction. Wear **10**, 199–213 (1967)
9. Pomeau, Y., Le Berre, M.: Critical speed-up vs critical slow-down: a new kind of relaxation oscillation with application to stick-slip phenomena (2011). arXiv:1107.3331v1
10. Burridge, R., Knopoff, L.: Model and theoretical seismicity. Bull. Seismol. Soc. Am. **57**, 341–371 (1967)
11. Dieterich, J.H.: A model for the nucleation of earthquake slip. In: Das, S., Boatwright, J., Scholz, C. (eds.) Earthquakes Source Mechanics. Geophys. Monogr. Ser., vol. 37, pp. 36–49. Am. Geophys. Union, Washington (1986)
12. Dieterich, J.H.: Earthquake nucleation on faults with rate- and state-dependent strength. Tectonophysics **211**, 115–134 (1992)
13. Scholz, C.H., Aviles, C.A., Wesnousky, S.G.: Scaling differences between large interplate and intraplate earthquakes. Bull. Seismol. Soc. Am. **76**, 65–70 (1986)
14. Marone, C., Vidale, J.E., Ellsworth, W.: Fault healing inferred from time dependent variations in source properties of repeating earthquakes. Geophys. Res. Lett. **22**, 3095–3098 (1995)
15. Marone, C.: The effect of loading rate on static friction and the rate of fault healing during the earthquake cycle. Nature **391**, 69–72 (1998)
16. Ben-David, O., Rubinstein, S.M., Fineberg, J.: Slip-stick and the evolution of frictional strength. Nature **463**, 76–79 (2010)
17. Gopalsamy, K., Leung, I.: Delay induced periodicity in a neural netlet of excitation and inhibition. Physica D **89**, 395–426 (1996)
18. Burić, N., Todorović, D.: Dynamics of delay-differential equations modeling immunology of tumor growth. Chaos Solitons Fractals **13**, 645–655 (2002)
19. De Sousa Vieira, M.: Chaos and synchronized chaos in an earthquake model. Phys. Rev. Lett. **82**, 201–204 (1999)
20. Erickson, B., Birnir, B., Lavallee, D.: A model for aperiodicity in earthquakes. Nonlinear Process. Geophys. **15**, 1–12 (2008)
21. Erickson, B.A., Birnir, B., Lavallée, D.: Periodicity, chaos and localization in a Burridge–Knopoff model of an earthquake with rate-and-state friction. Geophys. J. Int. **187**, 178–198 (2011)
22. Dieterich, J.H., Kilgore, B.D.: Direct observation of frictional contacts: new insights for state dependent properties. Pure Appl. Geophys. **143**, 283–302 (1994)
23. Rice, J.R.: Spatio-temporal complexity of slip on a fault. J. Geophys. Res. **98**, 9885–9907 (1993)
24. Lapusta, N., Rice, J.R.: Nucleation and early seismic propagation of small and large events in a crustal earthquake model. J. Geophys. Res. **108**, 1–18 (2003)

25. Szkutnik, J., Kawecka-Magiera, B., Kulakowski, K.: History-dependent synchronization in the Burridge–Knopoff model. Tribol. Ser. **43**, 529–536 (2003)
26. Engelborghs, K.: DDE-BIFTOOL v. 2.03: a MATLAB package for bifurcation analysis of delay differential equations (2000)
27. Engelborghs, K., Luzyanina, T., Samaey, G.: Technical report TW-330, Department of Computer Science, K.U. Leuven, Leuven, Belgium (2001)
28. Luzyanina, T., Enghelborghs, K., Ehl, S., Klenerman, P., Bocharov, G.: Low level viral persistence after infection with LCMV: a quantitative insight through numerical bifurcation analysis. Math. Biosci. **173**, 1–23 (2001)
29. Haegeman, B., Engelborghs, K., Roose, D., Pieroux, D., Erneux, T.: Stability and rupture of bifurcation bridges in semiconductor lasers subject to optical feedback. Phys. Rev. E **66**, 046216 (2002)
30. http://www.matjazperc.com/ejp/time.html
31. Belair, J., Campbell, S.A.: Stability and bifurcations of equilibria in a multiple delayed differential equation. SIAM J. Appl. Math. **54**, 1402–1424 (1994)
32. Campbell, S.A., Belair, J., Ohira, T., Milton, J.: Limit cycles, tori and complex dynamics in a second-order differential equation with delayed negative feedback. J. Dyn. Differ. Equ. **7**, 213–235 (1995)
33. Titchmarsh, E.C.: Theory of Functions. Oxford University Press, Oxford (1939)
34. Hale, J., Lunel, S.V.: Introduction to Functional Differential Equations. Springer, New York (1983)
35. Wiggins, S.: Introduction to Applied Nonlinear Dynamical Systems and Chaos. Springer, New York (2000)
36. Kuznetsov, Y.A.: Elements of the Applied Bifurcation Theory. Springer, New York (2004)
37. Ruelle, D., Takens, F.: On the nature of turbulence. Commun. Math. Phys. **20**, 167–172 (1971)
38. Ramana Reddy, D.V., Sen, A., Johnson, G.L.: Time delay induced death in coupled limit cycle oscillators. Phys. Rev. Lett. **80**, 5109–5112 (1998)
39. Campbell, S.A.: Time delays in neural systems. In: Jirsa, V.K., McIntosh, A.R. (eds.) Handbook on Brain Connectivity, pp. 65–90. Springer, Berlin (2007)
40. Prasad, A., Dhamala, M., Adhikari, B.M., Ramaswamy, R.: Amplitude death in nonlinear oscillators with nonlinear coupling. Phys. Rev. E **81**, 027201 (2010)
41. Newhouse, S., Ruelle, D., Takens, F.: Occurrence of strange axiom-A attractors near quasiperiodic flow on 7, $m > 3$. Commun. Math. Phys. **64**, 35–44 (1978)
42. Schmittbuhl, J., Vilotte, J.P., Roux, S.: Propagative macrodislocation modes in an earthquake fault model. Europhys. Lett. **21**, 375–380 (1993)